SAND2013-8913C

Evaluating Convergence of Reduced Order Models Using Nonlinear Normal Modes

Robert J. Kuether[1]
Matthew R. Brake[2]
&
Mathew S. Allen[1]

[1]*Department of Engineering Physics*
University of Wisconsin
Madison, WI 53706
rkuether@wisc.edu msallen@engr.wisc.edu
&
[2]*Component Science and Mechanics*
Sandia National Laboratories
Albuquerque, NM, 87185
mrbrake@sandia.gov

ABSTRACT

It is very expensive to integrate the response of a high order nonlinear system, such as a finite element model of a nonlinear structure, so a set of linear eigenvectors is often used as a basis in order to create a reduced order model (ROM). By augmenting the linear basis with a small set of discontinuous basis functions, ROMs of systems with local nonlinearities have been shown to compare well with the corresponding full order models. When evaluating the quality of a ROM, it is common to compare the time response of the model to that of the full order system, but the time response is a complicated function that depends on a predetermined set of initial conditions or external force. This is difficult to use as a metric to measure convergence of a ROM, particularly for systems with strong, non-smooth nonlinearities, for two reasons: 1.) the accuracy of the response depends directly on the amplitude of the load/initial conditions, and 2.) small differences between two signals can become large over time. Here, a validation metric is proposed that is based solely on the ROM's equations of motion. The nonlinear normal modes (NNMs) of the ROMs are computed and tracked as modes are added to the basis set. The NNMs are expected to converge to the true NNMs of the full order system with a sufficient set of basis vectors. This comparison captures the effect of the nonlinearity through a range of amplitudes of the system, and is akin to comparing natural frequencies and mode shapes for a linear structure. In this research, the convergence metric is evaluated on a simply supported beam with a contacting nonlinearity modeled as a unilateral piecewise-linear function. Various time responses are compared to show that the NNMs provide a good measure of the accuracy of the ROM. The results suggest the feasibility of using NNMs as a convergence metric for reduced order modeling of systems with various types of nonlinearities.

Keywords: Nonlinear normal modes, reduced order modeling, nonlinear dynamics.

1. Introduction

Reduced order modeling strategies for nonlinear finite element models provide a significant reduction in computational cost compared to direct numerical integration of the full order model. The general Galerkin approach uses a set of basis vectors that define the kinematics of the system, and produces a reduced set of equations in terms of generalized coordinates. Nonlinearities often require direct integration of the equations in order to analyze the behavior of a system to an input force. For example, long duration time simulations are used to generate the response to a random input in order to compute power spectral densities for life predictions of a geometrically nonlinear structure [1]. Such predictions with full order models containing many degrees-of-freedom require tremendous computational resources, and the cost (on the order of days and weeks) is typically out of reach for most systems of interest. Therefore, accurate reduction schemes become very appealing for analysis. A variety of model reduction strategies exist for nonlinear systems, such as models with localized nonlinearities [2-6], geometric nonlinearities [7-9], electro-mechanical interactions [10-12], and thermoelastic

effects [13, 14]. All of these reduction techniques have demonstrated that they can predict the behavior of the originating systems quite well when compared with either numerical or experimental data of the full system. In this paper, a novel validation metric is proposed for reduced order models (ROMs) of conservative, nonlinear systems based on the nonlinear normal modes (NNMs) of the reduced equations. The nonlinear mode is explored as a convergence metric for ROMs by tracking the NNMs as modes are added to the reduced basis set. With a sufficient number of modes in the basis set, the NNMs should converge to those of the full order model. This paper demonstrates the feasibility of this metric by drawing connections between the convergence of the NNM and the accuracy of the predicted response to two separate load cases: an impulsive force, and a random force input.

The appropriate reduction methodology for nonlinear finite element models depends on the type of nonlinearity in the physical model. This paper focuses on systems with impact nonlinearities, which are typically localized and can be modeled as discrete piecewise-linear functions. For localized nonlinearities, the reduction scheme originally developed by Segalman [5] is used, which proposed a reduced basis set comprised of linearized modes about some reference equilibrium (typically about a static equilibrium position), supplemented with a set of discontinuous basis functions. These discontinuous vectors, also referred to as Milman-Chu (MC) modes [15, 16], have been found to improve the accuracy of the ROM with comparison of the time histories to an impulsive load of the full order model [5, 17]. One question arises, though, when making such comparisons using a time response. Can two different models of the same nonlinear phenomenon be compared accurately with the response to a predetermined input? Is this a reasonable way to validate a ROM? Because of the impacts that occur, small differences in two separate models can become significant over time, resulting in divergent predictions. Over time, two separate models can ultimately predict responses that are 180 degrees out of phase with one another [3], making convergence measures prohibitively difficult. This characteristic is inherent in many non-smooth, nonlinear systems.

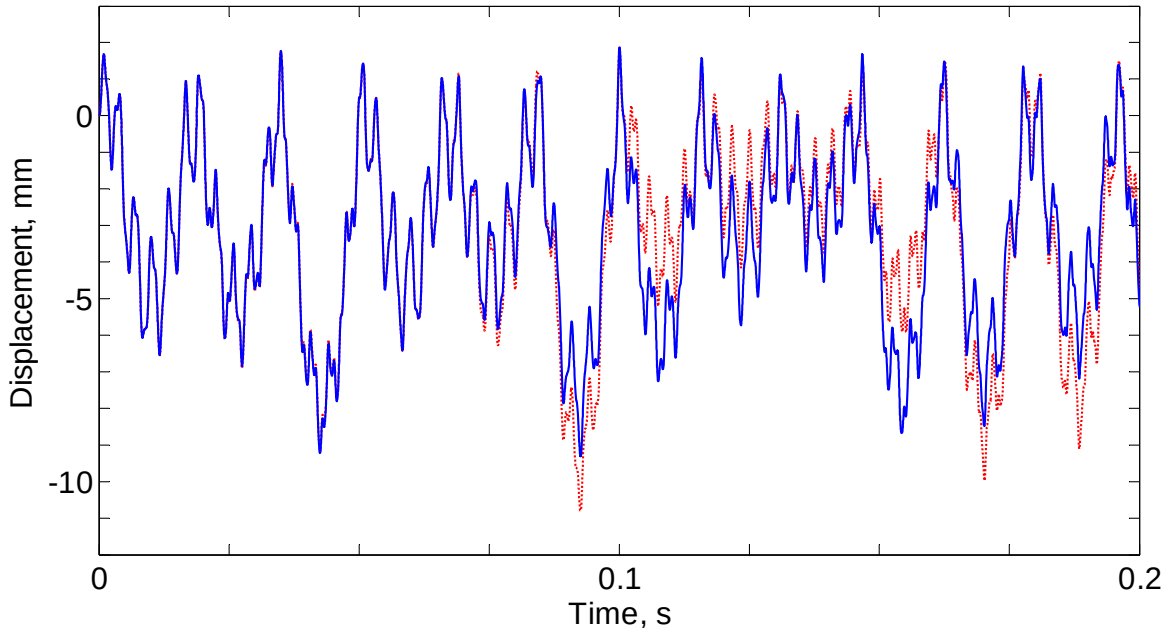

Figure1. Comparison of two similar models for a beam impacting an elastic stop.

In Fig. 1, the two models with contact nonlinearity are shown to diverge in their predicted results after about 0.1 seconds. This error originates in small differences between the two models observed across each impact, which compound over time and can lead to a phase shift, or a missed impact. While the time history may be very different due to the phase shift, this difference is not likely to significantly change the prediction of the system's failure threshold, since the two models still have similar response magnitudes and frequencies. On the other hand, the maximum response magnitude due to a certain input could be in agreement, but there might be many incorrect

system models that would predict the same maximum response magnitude for a certain input. Furthermore, either of these comparisons depends on the input and/or initial conditions. While a model might agree well with the measured response at one level of forcing input, this may not be the case for a different load level, as discussed in [18]. Computing the time history of the full order model for comparison may also be too computationally expensive for practical applications requiring large-scale models.

This work proposes instead to validate a ROM of a system based on the convergence of its NNMs, which are unique solutions of the undamped, unforced nonlinear equations of motion. A nonlinear normal mode is defined as a not-necessarily synchronous periodic solution to the conservative equations of motion [19, 20]. There exist at least N nonlinear normal modes for an N degree-of-freedom (DOF) system, and each NNM is described by a branch of solutions that typically reduces to the linearized modes at low energy. These branches can be represented in the frequency-energy plane, to show how the fundamental frequency and energy of the periodic motion changes as the amplitude of the free response evolves. These frequency-energy plots are used to characterize the dynamics of the system over a wide range of energy. This work proposes to compute a set of NNMs from the undamped ROM equations as modes are added to the basis set, and then to track the convergence of the NNMs to determine whether the ROM has converged, i.e. whether it accurately predicts the response frequencies and energy of the full order system. This approach is similar in spirit to a mesh refinement for a linear finite element model, where the natural frequencies are tracked and used to measure the convergence of the discretized model [21].

This comparison will only be useful if convergence of the NNMs of the system implies that the response of the system in the loading environment of interest will also be accurate. For example, the forced steady state response of the damped system at resonance, as shown in [22, 23], is identical to a NNM response, yet for other inputs the connection is not as well established. In this paper, the transient response is computed to a few different types of loadings to explore the connection between the convergence of the NNMs and the accuracy of the equations to predict the response to a predetermined loading environment.

The paper is outlined as follows. Section 2 reviews the model reduction strategy with discontinuous basis functions, as well as the theory underlying the nonlinear normal modes of a conservative, nonlinear system. In Section 3, the ROMs are generated for a simply supported beam with a local contact nonlinearity modeled as a unilateral piecewise-linear spring. The NNMs are computed from a set of ROMs with a successively increasing number of modes, and the convergence of the ROM model is evaluated based on the resulting NNMs. Following the convergence study, the ROMs are used to predict the response to an impulsive force with different load amplitudes, as well as a random force input. These results are compared to the response of the full order model, and used to evaluate the feasibility of using NNMs as a convergence metric. Conclusions are presented in Section 4.

2. Theoretical Development

Here it is assumed that the equations of motion have been discretized by the finite element method. The general representation for a conservative, N-DOF system is

$$\mathbf{M}\ddot{\mathbf{x}} + \mathbf{K}\mathbf{x} + \mathbf{f}_{NL}(\mathbf{x}) = \mathbf{f}(t), \tag{1}$$

where $\mathbf{M}$ and $\mathbf{K}$ are the $N \times N$ linear mass and stiffness matrices, respectively. The displacement, velocity and acceleration at each DOF are represented by the $N \times 1$ vectors $\mathbf{x}$, $\dot{\mathbf{x}}$, $\ddot{\mathbf{x}}$, respectively. The $N \times 1$ nonlinear restoring force vector $\mathbf{f}_{NL}(\mathbf{x})$ depends only on the displacement the system, as well as the conservative nonlinearity in the physical model.

2.1 Reduced Order Models with Local Nonlinearities

A Galerkin reduction procedure typically relies on the underlying linear, or linearized, mode shapes of the nonlinear dynamic system to form a basis set. The order of the system of equations is greatly reduced as the deformation space is approximated by a small set of shape vectors, significantly lowering the computational cost of numerical integration. The accuracy of these reduced equations depends greatly on the number of basis vectors used in the Galerkin approach, as well as the type of shape vectors used. When the system has localized

nonlinearities, such as piecewise-linear and cubic springs, prior works have found that the accuracy of the Galerkin approach can be increased dramatically by augmenting the linearized mode shapes with a set of discontinuous basis vectors [5]. These shapes [15, 16] permit completeness of the static response to the internal forces produced by the local nonlinearity.

The reduced basis requires the linearized modes of Eq. (1) about a reference equilibrium position $\mathbf{x}_0$, and are computed from the eigenvalue problem, which determines the natural frequencies ω and mode shapes ϕ,

$$\left[\mathbf{K}+\left.\frac{\partial \mathbf{f}_{NL}(\mathbf{x})}{\partial \mathbf{x}}\right|_{\mathbf{x}=\mathbf{x}_0}-\omega^2\mathbf{M}\right]\{\phi\}=\{\mathbf{0}\}. \tag{2}$$

The number of linearized modes to include has a significant influence on the accuracy of the resulting ROM. For linear systems, typically modes within 1.5 to 2.0 times the frequency band of interest are included. However, this range of modes may be insufficient for nonlinear systems since the nonlinearity can couple the underlying linear modes, resulting in the need to include higher frequency modes outside the prescribed frequency range of interest.

The set of linear basis vectors computed in Eq. (2) is augmented with a set of discontinuous basis vectors in order to satisfy the kinematic constraints at the location of the nonlinearity. These shapes are essentially static deformations that result from a self-equilibrating unit load applied to the associated DOF where the nonlinear element is located. Mathematically, the discontinuous basis vectors for the discretized system of equations in Eq. (1) are computed from the static problem

$$\mathbf{\Psi}=\left[\mathbf{K}+\left.\frac{\partial \mathbf{f}_{NL}(\mathbf{x})}{\partial \mathbf{x}}\right|_{\mathbf{x}=\mathbf{x}_0}\right]^{-1}\mathbf{B} \tag{3}$$

using the $N\times N_i$ Boolean matrix $\mathbf{B}$ that contains N_i nonlinear elements in the model. The j^{th} column in $\mathbf{B}$ is a vector of zeros except for the rows corresponding to the DOF where the j^{th} nonlinear element is located. An equal and opposite unit force is applied to these DOF, so the rows are filled with either a 1 or -1, depending on the orientation of the force.

The linear transformation between physical and generalized coordinates using m linearized mode shapes, and N_i discontinuous basis vectors is given by the following, where $\mathbf{\Phi}$ denotes the $N\times m$ matrix of linearized, mass normalized modes shapes and $\mathbf{\Psi}$ denotes the $N\times N_i$ set of discontinuous basis vectors.

$$\mathbf{x}=\mathbf{P}\mathbf{q}=\begin{bmatrix}\mathbf{\Phi} & \mathbf{\Psi}\end{bmatrix}\mathbf{q} \tag{4}$$

The transformation matrix $\mathbf{P}$ is orthnormalized with respect to the mass matrix, for example using a Gram-Schmidt procedure [3]. Substituting Eq. (4) into Eq. (1), and premultiplying by the transpose $(\,)^{\mathrm{T}}$ of $\mathbf{P}$, the reduced equations of motion become

$$\begin{aligned}\hat{\mathbf{M}}\ddot{\mathbf{q}}+\hat{\mathbf{K}}\mathbf{q}+\mathbf{P}^{\mathrm{T}}\mathbf{f}_{NL}(\mathbf{q})&=\mathbf{P}^{\mathrm{T}}\mathbf{F}(t)\\ \hat{\mathbf{M}}&=\mathbf{P}^{\mathrm{T}}\mathbf{K}\mathbf{P}\\ \hat{\mathbf{K}}&=\mathbf{P}^{\mathrm{T}}\mathbf{K}\mathbf{P}.\end{aligned} \tag{5}$$

Equation (5) is significantly less expensive to integrate than the full order system in Eq. (1), especially for high fidelity finite element models of realistic engineering structures. While these cost savings provide a significant advantage, the accuracy of the ROM must also be considered. If these equations do not accurately capture the physics of the original model from which it is defined, then they provide no utility for analysis. A convergence metric is proposed within this paper based on the nonlinear normal modes of the reduced equations. These NNMs are computed and tracked as linearized modes are added to the basis set, providing a metric to infer the validity of the reduced equations.

2.2 Nonlinear Normal Modes

A nonlinear normal mode is defined here as a not necessarily synchronous periodic solution to the conservative, nonlinear equations of motion. This extended definition by Vakakis, Kerschen and others [19, 20] allows for internal resonances, which are periodic motions but not synchronous, and occur when two or more modes interact. This new definition of a nonlinear mode provides a framework for the structural dynamicist to analyze and interpret the behavior of a nonlinear system from a geometric point of view. As the response amplitude of the NNM increases, the fundamental frequency and response evolve. For example, the NNM frequencies tend to increase (or decrease) if the nonlinearity is hardening (or softening) .

Unfortunately, NNMs lack two of the key properties that are associated with linear modal analysis: superposition and orthogonality. Superposition is a fundamental property of linear system theory and does not apply to nonlinear systems, and there is no useful orthogonality principle for NNMs to decouple the nonlinear equations of motion. The nonlinear modes are useful, though, since they form the backbone to the nonlinear forced response curves [19, 22, 23] of systems with smooth nonlinearities. The work in [24] used NNMs for system identification of an experimental beam with geometric nonlinearity. The freely decaying response of a lightly damped structure often closely follows an NNM branch as energy is dissipated, and this has been used to experimentally identify them [19]. Furthermore, NNMs have been exploited as an energy dependent model for a system in [25-27] in order to extend modal substructuring to geometrically nonlinear systems.

This work uses the pseudo-arclength continuation algorithm, developed originally by Peeters et al. [28], to compute the NNMs of a discretized system of equations, and hence the algorithm is briefly reviewed here. For the *N*-DOF system in Eq. (1) with $\mathbf{f}(t)=\mathbf{0}$, there exist *N* nonlinear normal modes that initiate at a linear (or linearized) mode at low energy, or low response amplitude. The NNM algorithm uses the shooting technique to find a set of initial conditions and integration period that result in a periodic, free response of the nonlinear equations of motion. A shooting function is defined

$$\mathbf{H}\left(T,\mathbf{x}_0,\dot{\mathbf{x}}_0\right)=\begin{Bmatrix}\mathbf{x}\left(T,\mathbf{x}_0,\dot{\mathbf{x}}_0\right)\\ \dot{\mathbf{x}}\left(T,\mathbf{x}_0,\dot{\mathbf{x}}_0\right)\end{Bmatrix}-\begin{Bmatrix}\mathbf{x}_0\\ \dot{\mathbf{x}}_0\end{Bmatrix}=\{\mathbf{0}\}, \tag{6}$$

where *T* is the integration period, and $\mathbf{x}_0$ and $\dot{\mathbf{x}}_0$ are the initial displacements and velocities, respectively. The system of equations must be integrated over a period *T* subject to the initial conditions $\mathbf{x}_0$ and $\dot{\mathbf{x}}_0$ to determine whether this set of variables produces a periodic response. A numerical tolerance ε is used as a threshold value

$$\frac{\left\|\mathbf{H}\left(T,\mathbf{x}_0,\dot{\mathbf{x}}_0\right)\right\|}{\left\|\begin{Bmatrix}\mathbf{x}_0\\ \dot{\mathbf{x}}_0\end{Bmatrix}\right\|}<\varepsilon\,. \tag{7}$$

When this condition is satisfied to a given tolerance, the solution is taken to be periodic and is defined as a NNM at a certain energy. A known periodic solution is uniquely defined by $\mathbf{x}_0$, $\dot{\mathbf{x}}_0$, and *T*, and is used with the pseudo-arclength continuation algorithm to predict a new periodic solution near the current one. (Continuation algorithms need an initial solution in order to generate a continuous branch, and the linear mode solutions at low energy provide an excellent starting point.) A step size controller determines the magnitude of the prediction step based on the number of iterations taken during the preceding correction steps.

As mentioned earlier, the NNMs form the backbone of the forced steady state response and give the response at resonance under certain conditions. Specifically, suppose a linear viscous damping term is added to Eq. (1)

$$\mathbf{M}\ddot{\mathbf{x}}+\mathbf{C}\dot{\mathbf{x}}+\mathbf{K}\mathbf{x}+\mathbf{f}_{NL}\left(\mathbf{x}\right)=\mathbf{f}\left(t\right). \tag{8}$$

In [23], Peeters, Kerschen, and Golinval found that if a multi-harmonic force is applied to the model that exactly cancels out the damping force (e.g. $\mathbf{C}\dot{\mathbf{x}}=\mathbf{f}(t)$), then a single NNM motion is isolated. Studies in [22, 23] found that a single-point, monoharmonic force can approximately excite the NNM motion along the backbone, or at the

peaks of the nonlinear forced response curves. Hence, if a model accurately captures an NNM then it will also accurately reproduce at least part of the nonlinear forced response curves at various amplitude levels.

The proposed procedure for using NNMs as a convergence metric begins by generating a set of ROMs with an increasing number of modes in the basis set. As with other convergence studies, additional modes in the basis should improve the ability of the ROM to capture the kinematics of the response. A set of NNMs are computed from these ROMs, which are selected to span a predetermined frequency range. Once all the NNMs are computed, the highest fidelity ROM is checked for convergence by comparing each of the NNMs to the lower fidelity models. It is assumed that if the NNMs of a ROM converge to those of the full model, then the reduced equations would be able to accurately predict the response to an arbitrary force input or initial condition. No formal proof yet exists to validate this statement; however, these branches capture solutions of the system for a range of response amplitudes, providing a significant improvement over validation with a time response.

3. Numerical Results

The convergence study is applied to a reduced order model of the nonlinear beam shown in Fig. 2. The linear, simply supported beam is modeled in Abaqus® using 40 B31 beam elements, resulting in a total of 119 DOF. The contact is modeled as a linear spring with a unilateral piecewise-linear function at a distance l_1 from the left support, with a spring stiffness of k and clearance a. When the spring is engaged, it applies an internal force in the transverse direction. This displacement dependent force results in a non-smooth, nonlinear system of equations. The spring in this example is located at the midpoint of the beam (l_1 = 4.5 inches), with a clearance of a = 0.0155 inch. The material and geometric properties of the nonlinear system in Fig. 2 are given in Table 1.

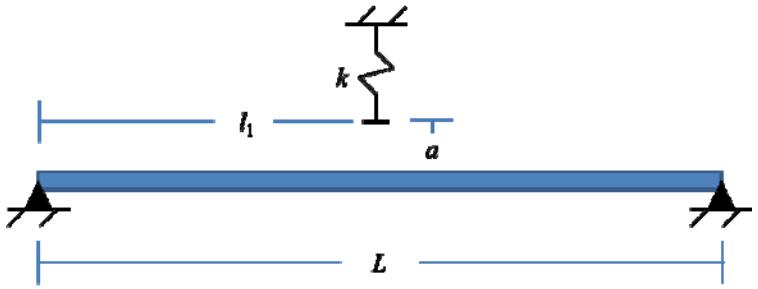

Figure 2. Schematic of simply supported beam with discrete contact nonlinearity.

Table 1. Material and geometric properties of the nonlinear beam model.

Property	Value
Young's Modulus	29,700 ksi
Poisons Ratio	0.28
Shear Modulus	11,600 ksi
Density	7.36E-4 lb-s^2/in^4
Length	9 inches
Width	0.5 inch
Thickness	0.031 inch
K_{eq}	9.7 lbf/inch
…	…
Spring Stiffness, k	200 lbf/inch
Spring Clearance, a	0.0155
Spring Location, l_1	4.5 inches

Prior to the convergence analysis, the first seven linear modes of the beam were computed, and the corresponding natural frequencies are listed in Table 2. Each is a low frequency bending mode, where the even mode numbers

are asymmetric shapes and the odd numbers are symmetric. Only the odd bending modes are used in the reduction scheme, since all of the even modes have nodal points at the impact location. Since the nonlinearity is localized to only a single DOF, only a single discontinuous basis vector is computed for each ROM, and is orthonormalized to the mass matrix. As a result, the augmented basis vector changes depending on which other linear modes are included in the basis set.

Table 2. Linear natural frequencies of simply supported beam.

Mode 1	Mode 2	Mode 3	Mode 4	Mode 5	Mode 6	Mode 7
34.8 Hz	139.4 Hz	313.8 Hz	558.2 Hz	872.7 Hz	1257.8 Hz	1713.7 Hz

3.1 Nonlinear Normal Mode Convergence

The nonlinear modes of various nonlinear ROMs are computed to study the convergence of the system in Fig. 2 as modes are added to the basis set. In this study, ROMs with mode [1], modes [1 MC], modes [1 3 5 MC] and modes [1 3 5 7 9 11 MC] were generated using the approach described in Section 2.1. The MC mode is the additional discontinuous basis vector that is used to improve the kinematics introduced by the internal force of the contacting spring, and the others are the mode numbers of the linear bending modes computed from the linear mass and stiffness matrix. The first, third and fifth NNMs (all symmetric) were computed from the ROMs, and the resulting frequency-energy plots are presented in Figs. 3-6. Each NNM initiates at the corresponding low energy, symmetric bending mode in Table 2, which are all between 0 and 1,000 Hz.

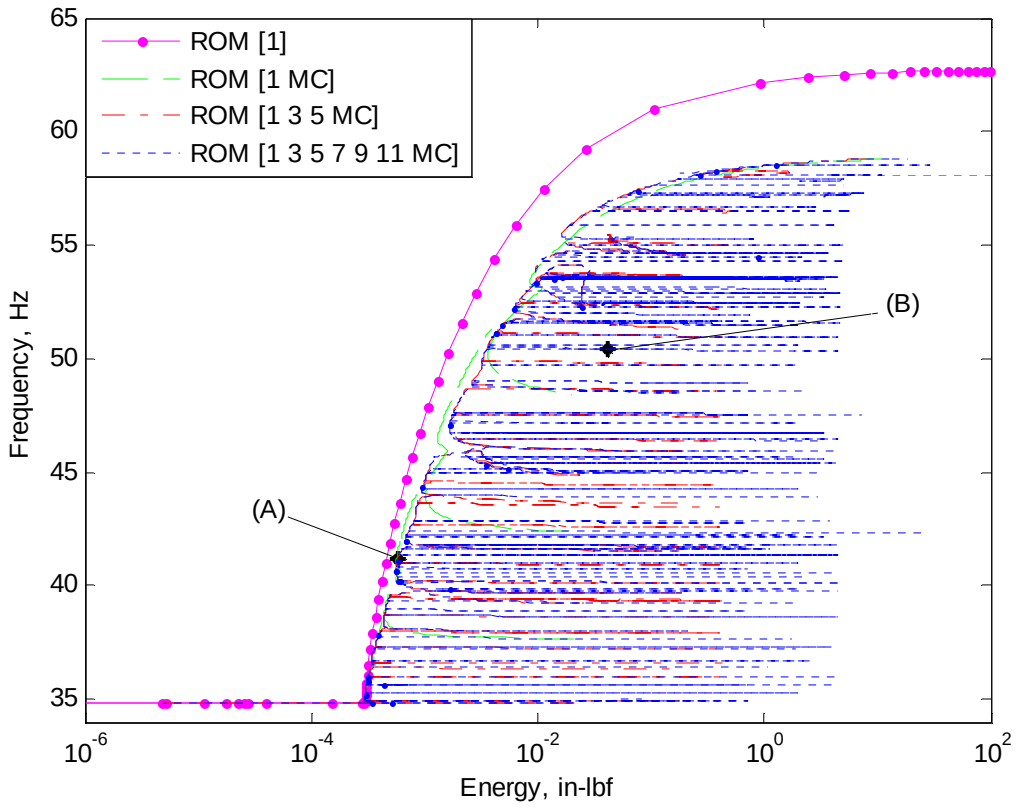

Figure 3. The first NNM computed for the (dotted magenta) ROM with mode [1], (dashed green) ROM with modes [1 MC], (dash-dot red) ROM with modes [1 3 5 MC], and (short dashed blue) ROM with modes [1 3 5 7 9 11 MC]. Time response of solutions (A) and (B) are plotted in Fig. 4.

The first NNM is initiated at the first linear mode with a frequency of 34.8 Hz, and is computed out to a 69% shift in fundamental frequency (with the 7-mode ROM). At low energy, the response amplitude is low enough that the

contacting spring is not engaged with the beam, and the periodic response is exactly that of the first linear bending mode. The range of linear response is seen by the straight line in the frequency-energy plane in Fig. 3. Each of the ROMs includes the first linear bending mode in the basis set, and therefore is able to exactly capture this portion of the branch. Once the midpoint amplitude of the first bending mode reaches the spring clearance (a = 0.0155 inch), the beam engages the spring, causing the periodic solutions to change. The transition from linear to nonlinear occurs at an energy of $3.0 \cdot 10^{-4}$ in-lbf, and the periodic responses stiffen (e.g. increase in frequency) due to the added stiffness of the contacting spring.

Two features of the NNM branch are observed in this nonlinear range: the backbone and the internal resonances. The internal resonances are the sharp peaks (with nearly constant frequency) along the branch that emanate from the backbone. These deviations from the backbone occur when two or more modes interact, and exchange energy with other nonlinear modes of the system. The plots in Fig. 4 show the time response of the two NNM solutions marked (A) and (B) in Fig. 3 for the ROM with modes [1 3 5 7 9 11 MC]. The response of solution (A) oscillates with a fundamental frequency of about 41.2 Hz predominantly in the shape of the first bending mode. Through one period of response, Figs. 4a and 4b show that this NNM solution contains higher order harmonics as well as slight contributions of higher order bending modes. Solution (B) shows a periodic solution of the first NNM along one of its many internal resonances, occurring at a frequency of about 50.4 Hz. This is a 1:34 internal resonance with the 7th bending mode, meaning that the 7th mode oscillates at a frequency 34 times the frequency of the first bending mode. The deformation shapes in Fig. 4c highlight the complicated response throughout different snapshots of the time history, with strong contributions from the 1st and 7th mode.

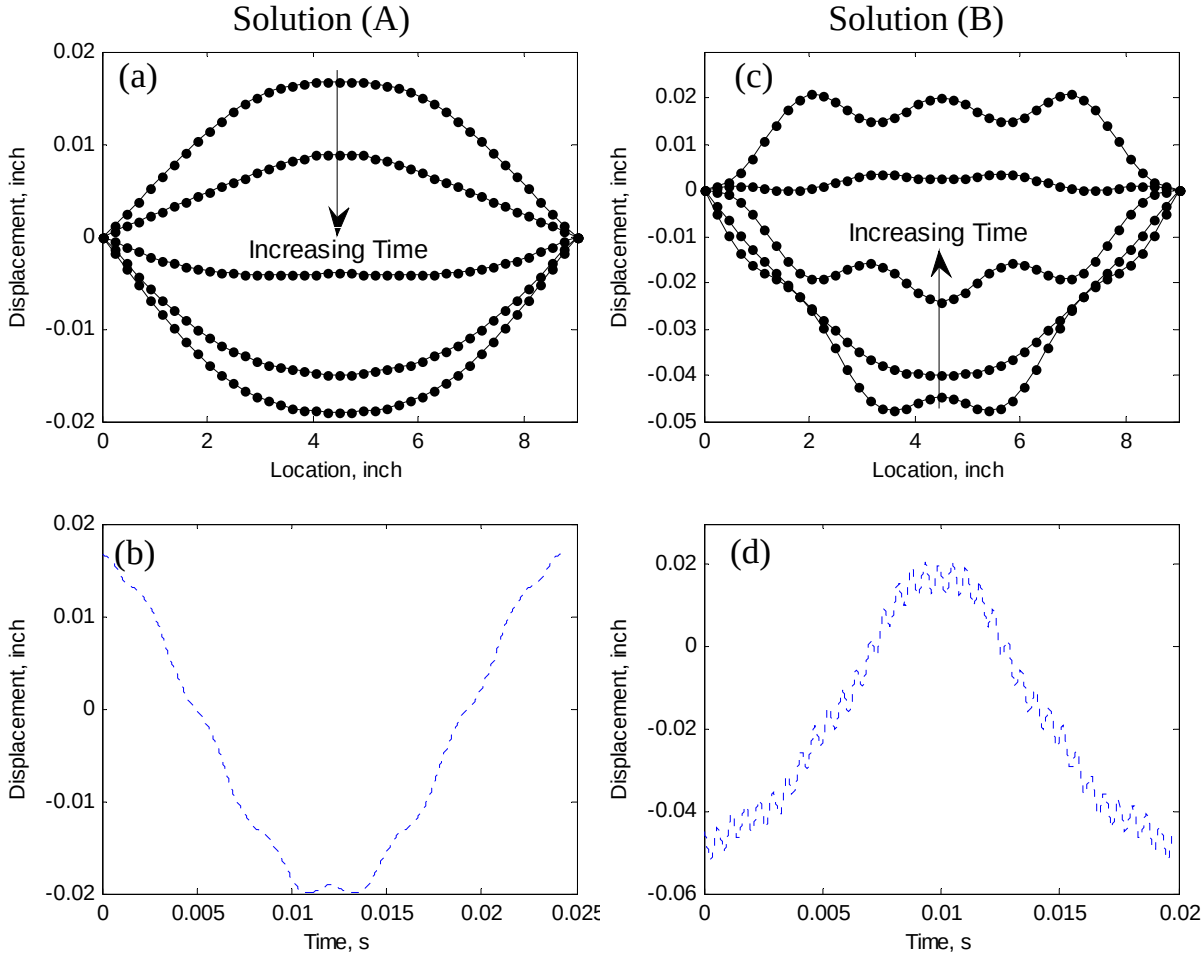

Figure 4. Time history of NNM solutions (A) and (B) in Fig. 3 for the ROM with modes [1 3 5 7 9 11 MC]. Plots (a) and (c) show the beam deflection shape at different snapshots in time, and plots (b) and (d) show the time history of the contacting DOF over one period.

The ROM with mode [1] only computes the backbone of the first NNM in Fig. 3, but does not have any internal resonances since these only occur with multi-DOF systems. The higher fidelity ROMs with modes [1 3 5 MC] and modes [1 3 5 7 9 11 MC] show an abundance of these tongues which are very difficult to compute with the pseudo-arclength continuation algorithm. During the computation of this NNM, a very small stepsize is required in order to resolve these sharp features. If the step sizes are too large, the prediction steps can potentially skip over the internal resonance, or jump to other branches that are not a continuation of the current branch. For this reason, it is not certain that the first NNM in Fig. 3 shows all of the internal resonances that are possible with these higher fidelity ROMs.

The first NNM from the ROM with only mode [1] captures the linear solution at energies below $3.0 \cdot 10^{-4}$ in-lbf, but does not accurately capture the backbone in the nonlinear range. For example, at an energy level of 5.0 in-lbf, this ROM predicts a frequency of 62.5 Hz, whereas the other ROMs predict 58.7 Hz, an error of 6.5%. On the other hand, the [1 MC] ROM captures the backbone quite accurately, revealing that the static effect of the nonlinearity is all that was needed to describe this feature. On the other hand, the ROM with modes [1 MC] only computed 3 internal resonances, which is significantly fewer than the number computed with the higher fidelity ROMs. This reveals that the contacting spring is coupling higher order linear modes into the response, so several additional modes are needed in the basis set to accurately capture the internal resonances. The backbone appears to be converged to high precision with the [1 3 5 MC] and [1 3 5 7 9 11 MC] mode ROMs. However, the internal resonances of these ROMs have not yet converged, as the 7-mode ROM still introduces many new tongues along the backbone and few if any agree with those of the 4-mode ROM. This comparison has revealed that a relatively simple model can accurately capture the basic frequency-energy dependence of this system, but tremendously more effort will be needed if internal resonances must also be accurate.

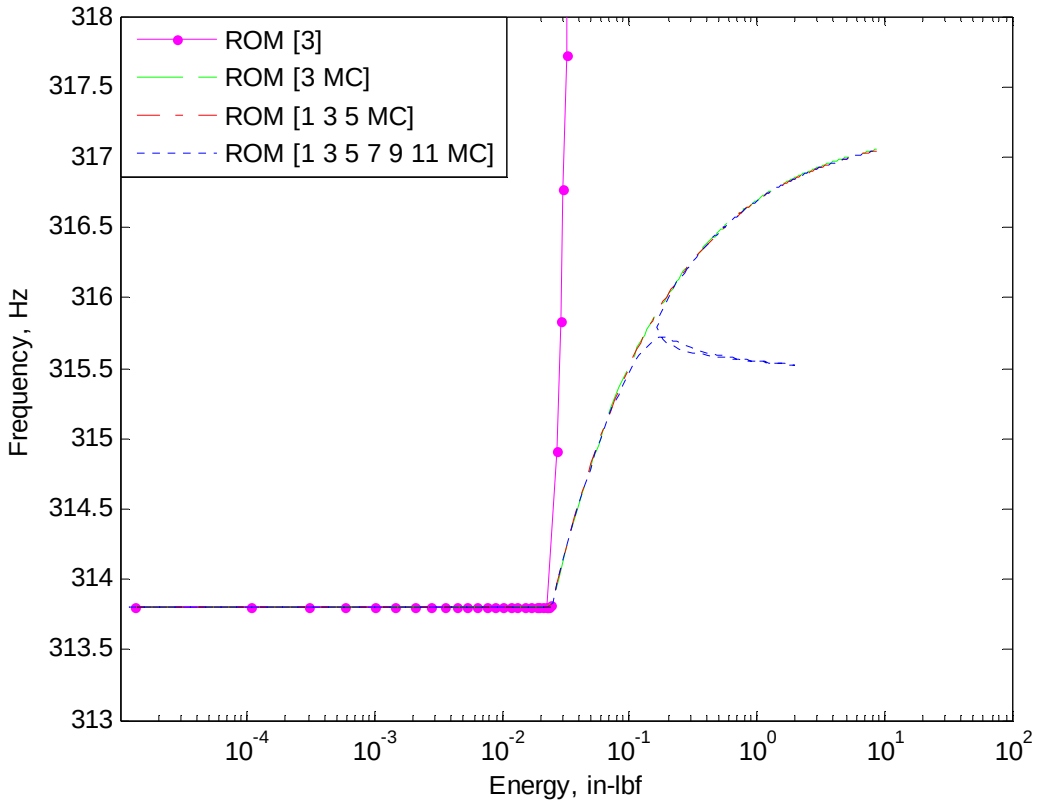

Figure 5. The third NNM computed for the (dotted magenta) ROM with mode [1], (dashed green) ROM with modes [1 MC], (dash-dot red) ROM with modes [1 3 5 MC], and (short dashed blue) ROM with modes [1 3 5 7 9 11 MC].

The third NNM is plotted in Fig. 5 for ROMs generated with mode [3], modes [3 MC], modes [1 3 5 MC], and modes [1 3 5 7 9 11 MC]. The third NNM has the same features as the first NNM in Fig. 3, but now there is only one internal resonance. The nonlinear region of the third NNM begins at an energy of $2.4 \cdot 10^{-4}$ in-lbf; below this the beam oscillates in exactly the third bending mode with a frequency of 313.8 Hz. Above $2.4 \cdot 10^{-4}$ in-lbf, the spring is engaged and causes the fundamental frequency of the motion to increase. The third NNM has a frequency shift of about 1.0 %, which is significantly less than that of the first NNM. Again, the ROM computed with mode [3] does not accurately calculate the backbone, although in this case the 1-mode model is far too stiff. The accuracy of this ROM improves greatly when one discontinuous basis vector is added to this ROM; adding additional modes to the ROM does not significantly change the backbone. However, as the model order is increased, there is an internal resonance that occurs at 315.8 Hz. This is only computed with the ROM with modes [1 3 5 7 9 11 MC]. This internal resonance is a 1:9 interaction with the 9th mode of the system, and hence cannot be captured unless the 9th mode is included in the basis set. Other internal resonances may also be introduced as more modes are added, but this will not be pursued further in this work.

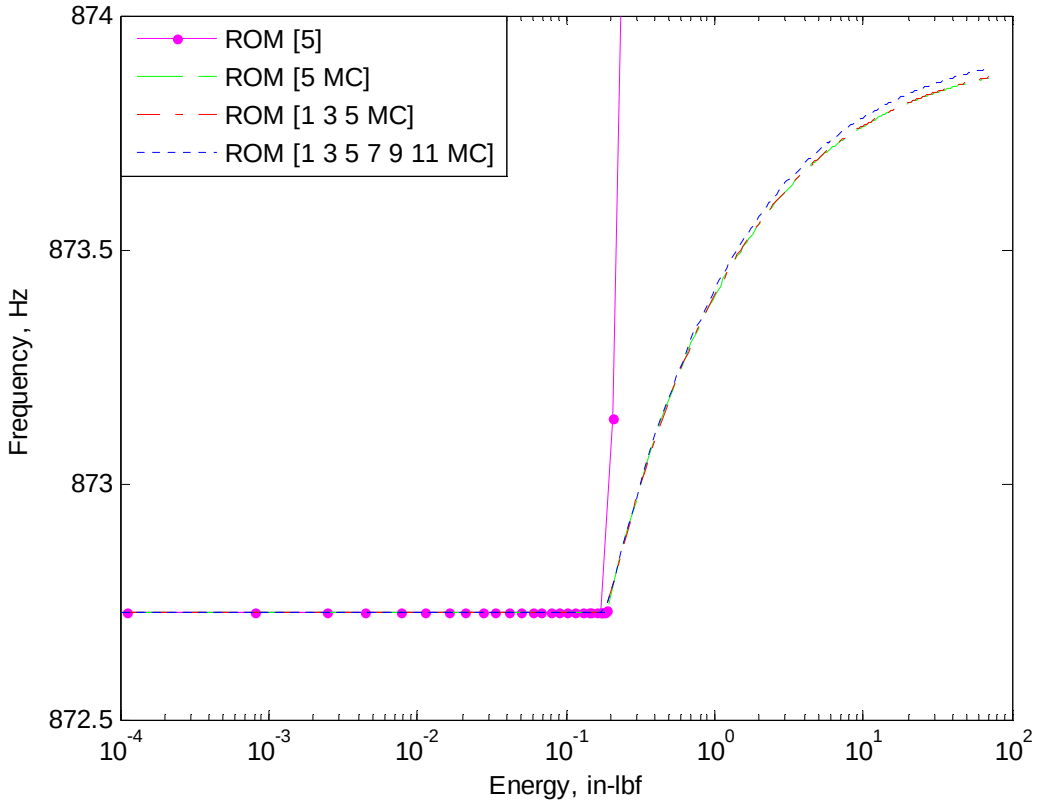

Figure 6. The fifth NNM computed for the (dotted magenta) ROM with mode [1], (dashed green) ROM with modes [1 MC], (dash-dot red) ROM with modes [1 3 5 MC], and (short dashed blue) ROM with modes [1 3 5 7 9 11 MC].

The nonlinear range of the fifth NNM in Fig. 6 begins at an energy level of 0.19 in-lbf, and has a total frequency shift of only 0.1% for the highest fidelity ROM that is used here. None of the ROMs predict an internal resonance in this fifth NNM over this energy range. The ROM with mode [5] alone appears to be very stiff compared to higher fidelity ROMs, consistent with the behavior of other NNMs. There is practically no difference between the backbone of the ROMs with modes [5 MC] and [1 3 5 MC], but the ROM with modes [1 3 5 7 9 11 MC] causes the backbone to shift slightly to higher frequency. In order to determine whether this backbone is converging, additional modes would need to be added to the basis set.

The comparisons presented so far reveal that in some cases adding additional modes to the basis set introduces new dynamics to the system, such as an additional internal resonance, while in other cases they simply improve

the accuracy of the response (e.g. when the model is augmented from [3] to [3 MC]). In the results shown here, the backbones of the first and third NNM appear to converge with the 7-mode ROM, but the internal resonances are not yet converged. Due to the complexity of the internal resonances, and the potentially infinite number of these solutions, one might ask how important these are to the accuracy of the ROMs for other predictive purposes (e.g. solutions to a forced response). Do these internal resonances manifest themselves in the response?

This question was addressed to a certain extent in a recent paper by Ardeh & Allen [29]. In that paper, the response of a 2DOF nonlinear system was studied in detail, revealing that many other branches of solutions exist with much lower fundamental frequencies than the linear modes. These solutions form manifolds in the state space that are tangent to the fundamental manifolds. Hence, a response on one manifold can easily travel onto (or along) another. This, and the erratic convergence of the first NNM presented above, suggest that the transient response of this system may be quite difficult to predict with great precision. In the following two sections the transient response is computed for a few different loadings in order to explore the correlation between the transient response computed by each ROM and their underlying NNMs.

3.2 Impulse Loading Verification

The first load considered is an impulsive load, modeled by a half-sine impulse in time. Spatially, the impulse is given the *shape of the first linear bending mode*, such that $\mathbf{f}(t) = \mathbf{M}\phi_1 A g(t)$, and g(t) is a half-sine impulse over a short time duration with some amplitude *A*. This load is chosen in order to excite the structure near the first NNM branch, where the characteristics of the first NNM should be most strongly manifest. The half-sine impulse is applied to the beam for a duration of 1 ms, with various peak amplitudes *A* to excite the structure to different energy levels. All initial conditions are set to zero. The response is integrated over 1.0 second with 10^7 time steps using an implicit HHT α method described in [30], with α =0 such that no numerical damping is added to the response. No damping is added to the equations of motion either, since the nonlinear modes used here to measure convergence are solely based on the conservative system. It should be noted that the undamped case is likely the worst possible scenario since error to small differences will grow in time, whereas damping cause these differences to dissipate.

To assess the suitability of the models for failure prediction, the root mean square (RMS) value of the midpoint displacement, over 1.0 second of undamped response, is calculated for each ROM. The maximum midpoint displacement is also found. The latter might be a metric of interest if brittle failure is expected due to a blast, while the former might be used to assess the fatigue damage incurred due to the forcing. The results for different system energy levels are compared in Tables 3 and 4.

Table 3. RMS value of midpoint displacement for various levels of excitation to a half-sine impulse in the shape of the first linear bending mode.

Load Case	ROM [1]	ROM [1 MC]	ROM [1 3 5 MC]	ROM [1 3 5 7 9 11 MC]	Full
E = $1.8\cdot10^{-4}$ in-lbf	$8.61\cdot10^{-3}$ in	$8.61\cdot10^{-3}$ in	$8.61\cdot10^{-3}$ in	$8.61\cdot10^{-3}$ in	$8.61\cdot10^{-3}$ in
E = $2.0\cdot10^{-3}$ in-lbf	$2.54\cdot10^{-2}$ in	$2.49\cdot10^{-2}$ in	$1.61\cdot10^{-2}$ in	$1.51\cdot10^{-2}$ in	$1.50\cdot10^{-2}$ in
E = $5.0\cdot10^{-2}$ in-lbf	0.133 in	0.129 in	0.0711 in	0.0699 in	0.0688 in
E = 0.76 in-lbf	0.525 in	0.507 in	0.421 in	0.414 in	0.414 in

Table 4. Maximum value of midpoint displacement for various levels of excitation to a half-sine impulse in the shape of the first linear bending mode.

Load Case	ROM [1]	ROM [1 MC]	ROM [1 3 5 MC]	ROM [1 3 5 7 9 11 MC]	Full
E = $1.8\cdot10^{-4}$ in-lbf	$1.21\cdot10^{-2}$ in	$1.21\cdot10^{-2}$ in	$1.21\cdot10^{-2}$ in	$1.21\cdot10^{-2}$ in	$1.21\cdot10^{-2}$ in
E = $2.0\cdot10^{-3}$ in-lbf	$4.05\cdot10^{-2}$ in	$4.05\cdot10^{-2}$ in	$3.84\cdot10^{-2}$ in	$3.92\cdot10^{-2}$ in	$3.92\cdot10^{-2}$ in
E = $5.0\cdot10^{-2}$ in-lbf	$2.03\cdot10^{-1}$ in	$2.04\cdot10^{-1}$ in	$1.94\cdot10^{-1}$ in	$1.88\cdot10^{-1}$ in	$1.85\cdot10^{-1}$ in
E = 0.76 in-lbf	0.786 in	0.792 in	0.778 in	0.762 in	0.762 in

For the response at low energy (E = $1.8\cdot10^{-4}$ in-lbf), the maximum displacement in Table 4 for each model is 0.0121 inch, which is below the contact clearance of *a*=0.0155 inch. The system responds purely in the first mode

to this loading, and all of the models are in perfect agreement. Knowing the system energy of the response, the frequency-energy plot of the first NNM in Fig. 3 shows that the system will respond in the linear range. The higher energy load cases in Tables 3 and 4, however, show that the system energy of each response is within the nonlinear range of the first NNM. The different load levels are explored since the system behavior depends on the displacement amplitude.

The ROMs with mode [1] and modes [1 MC] do not accurately predict the RMS and maximum displacements of the full order model. On the basis of the first NNM, each of these ROMs is determined to need additional modes in order to capture the number and density of internal resonances exhibited in the real system. The mode [1] ROM showed considerable error in the backbone while the [1 MC] ROM captured it reasonably well. All of this confirms that the internal resonances do play an important role in the transient response. It is also interesting to note that the 4-mode and 7-mode ROMs predict the RMS and maximum displacements quite accurately for each load case. In fact, the ROM with modes [1 3 5 7 9 11 MC] agrees very well with the full order model in the nonlinear range, except perhaps when the system energy is $E = 5.0 \cdot 10^{-2}$ in-lbf, where the ROM overpredicted the RMS displacement by 1.5%, and the maximum displacement by 1.6%. Hence, this ROM is quite acceptable even though it could not be assured that its first NNM had converged to the point that it predicted all of the system's internal resonances accurately. The internal resonances represent manifolds in the state space that connect different linear modes; perhaps the ROMs need only capture the location (in terms of frequency and energy) and the density of the resonances in order to allow energy to propagate correctly and hence to predict the RMS and maximum displacement accurately.

The first 0.5 seconds of the displacement response at the center of the beam (the DOF where contact occurs) for each load case is plotted in Fig. 7 for the full order model, and two of the ROMs (low and high fidelity), both of which include the augmented discontinuous basis vector. The ROM with modes [1 MC] overpredicts the amplitude of the response for all cases in the nonlinear region (Fig. 7b-7d), and appears to be dominated by a single frequency.

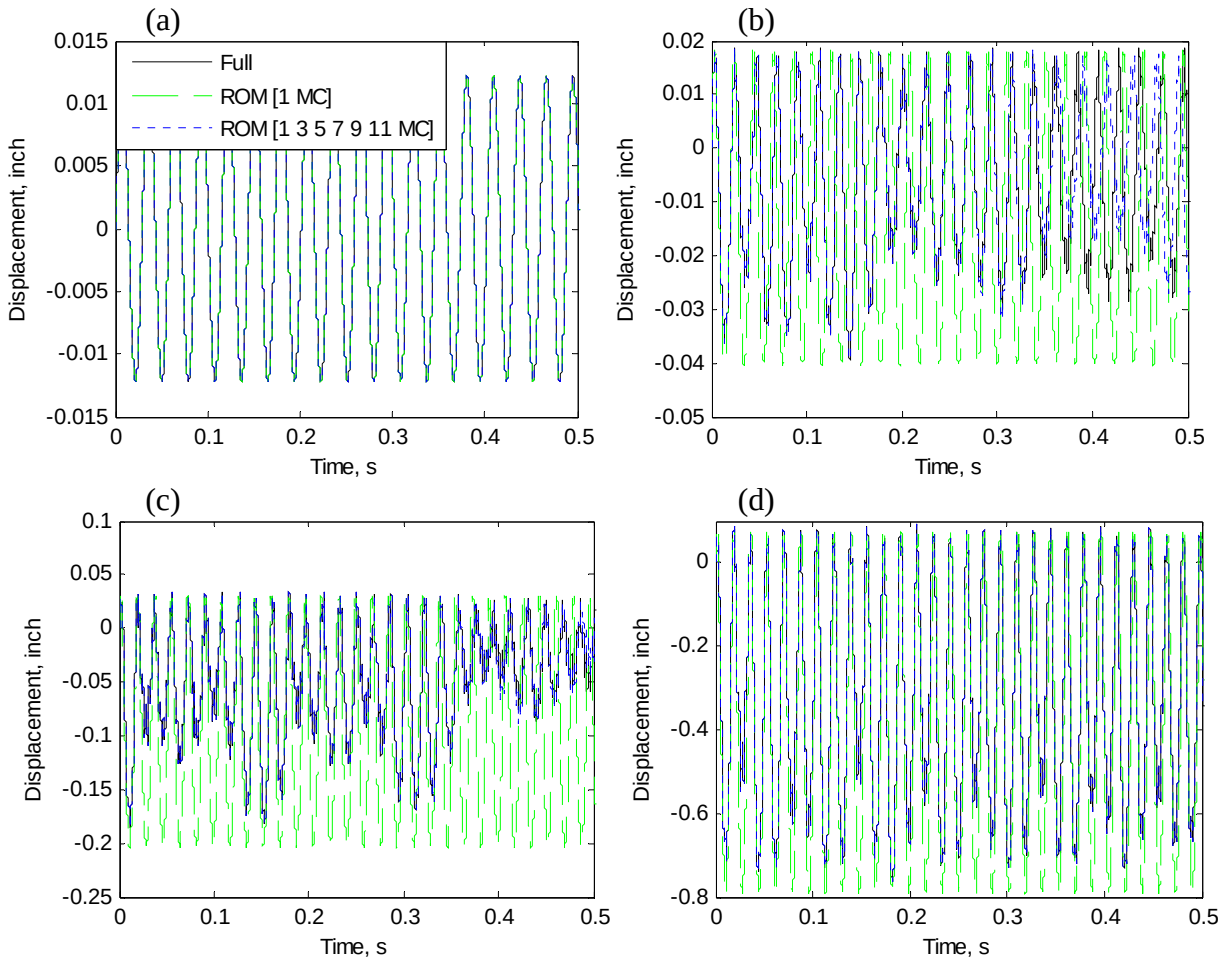

Figure 7. Response of contacting DOF due to a half-sine impulse in the shape of the first linear mode with system energy of (a) $E = 1.8 \cdot 10^{-4}$ in-lbf, (b) $E = 2.0 \cdot 10^{-3}$ in-lbf, (c) $E = 5.0 \cdot 10^{-2}$ in-lbf, and (d) $E = 0.76$ in-lbf. (Solid black) full order model, (dashed green) ROM with modes [1 MC], and (short dashed blue) ROM with modes [1 3 5 7 9 11 MC].

In contrast, the ROM with modes [1 3 5 7 9 11 MC] closely follows the response predicted by the full model, capturing the higher harmonics and the relative amplitude of the displacement, although the predicted response does have a significant phase error after about 0.3 seconds. As discussed earlier, this divergence is a common feature of systems with non-smooth nonlinearities. The system energy for this response is $E = 2.0 \cdot 10^{-3}$ in-lbf, and remains at that energy since no damping is included in the models. The first NNM in Fig. 3 shows many internal resonances at $E = 2.0 \cdot 10^{-3}$ in-lbf, suggesting that the system could travel along one of these manifolds and pump energy into another mode of the system, as was observed in the transient responses in [29]. Since the 7-mode ROM does not appear to converge at all of the internal resonances, the response that it predicts may travel along other nearby paths potentially transferring energy to different nonlinear modes and ultimately causing the time response to diverge.

It is interesting to point out that Figure 7d shows that at $E = 0.76$ in-lbf , the signals between the full model and the ROM with modes [1 3 5 7 9 11 MC] stay in phase over time, and appear to be in very good agreement. Figure 3 shows that, at this energy level, the backbone of the first mode has leveled off and there are perhaps fewer internal resonances that can come into the path of the system; perhaps this causes the response to be more likely to be captured on the manifold described by that backbone and to oscillate at almost a fixed frequency. Indeed, even the [1 MC] ROM does quite a good job at predicting the maximum and (to a lesser extent) RMS amplitudes and the frequency content in the response, further reinforcing the idea that the backbone is more important than the internal resonances at this energy level.

These comparisons have shown that, although the response of this system shows vastly different character at different energy levels, that its response is intimately connected to its nonlinear modes. Hence, a reduced order model that captures its nonlinear modes accurately is likely to correctly predict its response over the corresponding range of energy.

3.3 Random Loading Verification

The ROMs are now compared to the full order model using the response to a random force applied at the midpoint of the beam, only in the transverse direction. A linear damping model is included in the reduced and full order equations, based on mass and stiffness proportional damping (e.g. $\mathbf{C} = \alpha\mathbf{M} + \beta\mathbf{K}$), with α and β chosen so that the first and third modes of the linear beam have modal damping ratios of 0.005. The linear damping matrix for the ROMs is derived from this diagonalizable damping matrix. The lightly damped beam is forced using a broadband, Gaussian random input with zero mean and a standard deviation of σ. The input is filtered using an 8^{th} order Butterworth filter with a cutoff frequency of 1,000 Hz, in order to excite (at least) the first three symmetric modes of the system. Figure 8 shows the autospectrum of the midpoint displacement for a forcing level with a standard deviation of σ = 0.1 lbf.

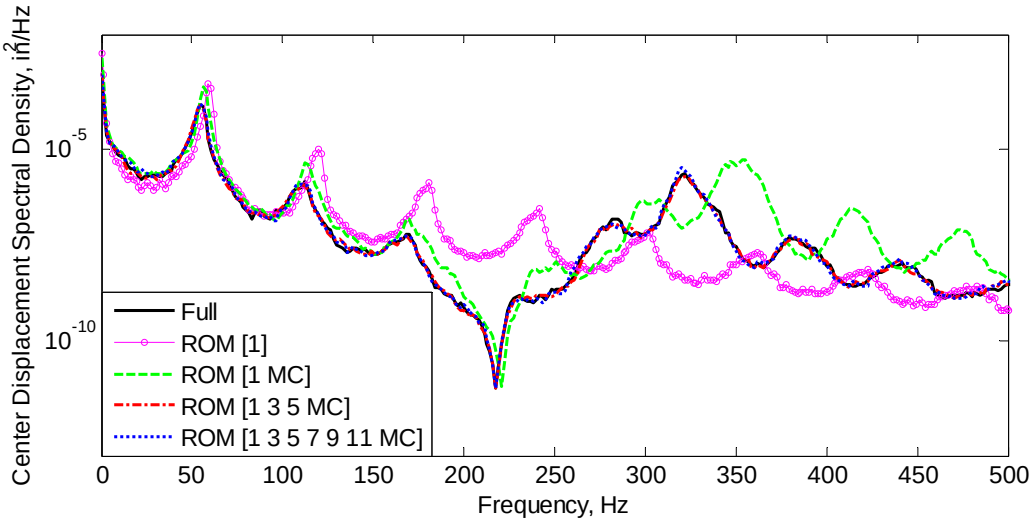

Figure 8. Autospectrum of the midpoint transverse displacement to a random force input with a standard deviation of σ = 0.1 lbf.

All of the models show that the response is dominated by a peak around 54 Hz, which can be attributed to the first nonlinear mode of vibration. The harmonics of this peak occur at 108.8 Hz, 168 Hz, and so forth, and are especially prominent in the response of the mode [1] ROM. Since this 1-mode ROM does not have any internal resonances in the first NNM, these harmonics must result from the response about the first mode of the system. Some of those peaks are visible in the response of the higher order ROMs, although overall the mode [1] poorly predicts the frequencies of the peaks in Fig. 8. Furthermore, while it does predict that the dominant frequencies will be near 54 Hz, the model is stiffer than the true system, as inferred based on its NNM. It also over-predicts the response near the first mode, presumably because it doesn't allow energy to transfer to any other modes.

The [1 MC] model improves on the frequency content near the 54 Hz resonance peak (as expected based on its NNM backbone), but it still over-predicts the amplitude of the response by a significant amount. It seems that the first mode exchanges energy with the third mode and hence the model must include that mode (and perhaps the corresponding internal resonances) in order to predict the response level accurately.

The higher fidelity ROMs with modes [1 3 5 MC] and [1 3 5 7 9 11 MC] agree very well with the results from the full order model. The increase in frequency (or stiffness) for the first peak occurs due to the engagement of the contacting spring, just as the backbone of the first NNM increases in frequency with higher response levels. At lower force levels, this first peak shifts to a lower frequency (not shown here for brevity). The autospectrum in Fig. 8 suggests that the convergence of the backbone is the most important feature of accurately predicting the

response to a random load, since the 4-mode and 7-mode ROM predict nearly the same response as the full order model. However, the internal resonances are important to some degree as well. For example, one could create a 7-mode model that neglects the coupling between the modes, and while such a model might accurately capture the backbones it would not predict the response amplitudes very accurately. This was illustrated in the cases shown in [31]. Even then, it appears that for a system like this it is not critical that each internal resonance converge, as long as the system has some internal resonances at the energy level of interest. Further research will be needed to determine whether the number of internal resonances is critical or if there is some other feature that they must capture to reproduce the correct response.

4. Conclusion

A novel approach is proposed in this paper to study the convergence of a reduced order model of a system with nonlinearity. The nonlinear normal modes are computed for a ROM with an increasing number of basis vectors, and tracked in order to observe how the nonlinear modes converge as additional basis vectors are added. The NNMs readily describe many periodic solutions of the undamped, unforced system as a function of system energy (or response amplitude), and seem to characterize the solution space of the system more effectively than the time history obtained in response to a predetermined initial condition or applied force. The methodology was demonstrated on a system with an impact nonlinearity, whose non-smooth characteristics have made validation efforts in the time domain difficult due to issues of divergence between two time signals. The ROMs of a beam with a single contacting spring were generated using the approach in [5], and the NNMs of these ROMs were computed using the pseudo-arclength continuation algorithm in [28].

The first NNM of the nonlinear beam appeared to have converged along the main backbone with either a 4- or 7-mode ROM, but the internal resonances were not yet converged. The difficulty in computing the tongues, and the large number of these solutions made it difficult to evaluate the convergence of the system without studying higher order ROMs. Regardless, the addition of modes to the basis exploited the effect on the dynamics of the system, such as the convergence of the solutions along the backbone and internal resonances. The third and fifth NNMs showed similar behavior. The ROMs studied for convergence were then verified by comparing the time histories to an impulsive load in the shape of the first linear mode, and to a random external force. The impulse response showed that the 7-mode ROM accurately captured the amplitude and frequency of the response for a range of excitation amplitudes. Over time, the signals between the full model and 7-mode ROM began to diverge, even though the RMS and maximum displacement results were in good agreement. The convergence along the backbone seems to contribute to the accuracy of the response, but the internal resonances are suspected to contribute to the divergence of the signal over time. The response to a random excitation showed that the 4-mode and 7-mode ROM accurately predict the response of the system. These models required higher order modes to accurately capture the backbone of the first NNM and allow the transfer of energy to higher order modes during the response to a random input.

Although the procedure studied here was demonstrated on a conservative system, other definitions of NNMs exist for damped systems [32, 33], and a similar convergence study could be taken. This convergence analysis is independent of the model reduction technique, or the method used to compute the NNMs. For example, systems with damping nonlinearities (e.g. jointed stuctures [34]) would require a different definition/computation technique of an NNM. This paper demonstrated the general convergence procedure on a system with impacting nonlinearities, whose nonlinear modes were complicated solutions of the system. One discovery is the abundance of internal resonances for these types of nonlinearities over the range of the first NNM. In future work, the authors would like to further explore the importance of these internal resonances, and look at the stability of these solutions [19]. By further identifying the portion of the NNM that is stable, further insights will be sought that could help distinguish whether an internal resonance is important for convergence.

Acknowledgements

This work was partially conducted at Sandia National Laboratories. Sandia is a multi-program laboratory operated under Sandia Corporation, a Lockheed Martin Company, for the United States Department of Energy under Contract DE-AC04-94-AL85000.

References

[1] R. W. Gordon and J. J. Hollkamp, "Reduced-Order Models for Acoustic Response Prediction," Air Force Research Laboratory (AFRL), Wright-Patterson Air Force Base, OH AFRL-RB-WP-TR-2011-3040, 2011.

[2] P. Avitabile and J. O'Callahan, "Efficient techniques for forced response involving linear modal components interconnected by discrete nonlinear connection elements," *Mechanical Systems and Signal Processing*, vol. 23, pp. 45-67, 2009.

[3] M. R. Brake and D. J. Segalman, "Modelling localized nonlinearities in continuous systems via the method of augmentation by non-smooth basis functions," *Proceedings of the Royal Society A: Mathematical, Physical and Engineering Science*, vol. 469, October 8, 2013 2013.

[4] Z.-Q. Qu, "Model Reduction for Dynamical Systems with Local Nonlinearities," *AIAA Journal*, vol. 40, pp. 327-333, 2002/02/01 2002.

[5] D. J. Segalman, "Model reduction of systems with localized nonlinearities," *Transactions of ASME. Journal of Computational and Nonlinear Dynamics*, vol. 2, pp. 249-66, 2007.

[6] T. Zheng and N. Hasebe, "An Efficient Analysis of High-Order Dynamical System with Local Nonlinearity," *Journal of Vibration and Acoustics*, vol. 121, pp. 408-416, 1999.

[7] M. Brake and D. Segalman, "Nonlinear model reduction of von Kármán plates under quasi-steady fluid flow," *AIAA Journal*, vol. 48, pp. 2339-2347, 2010.

[8] J. J. Hollkamp, R. W. Gordon, and S. M. Spottswood, "Nonlinear modal models for sonic fatigue response prediction: a comparison of methods," *Journal of Sound and Vibration*, vol. 284, pp. 1145-63, 2005.

[9] M. P. Mignolet, A. Przekop, S. A. Rizzi, and S. M. Spottswood, "A review of indirect/non-intrusive reduced order modeling of nonlinear geometric structures," *Journal of Sound and Vibration*, vol. 332, pp. 2437-2460, 2013.

[10] L. D. Gabbay and S. D. Senturia, "Computer-aided generation of nonlinear reduced-order dynamic macromodels. I. Non-stress-stiffened case," *Microelectromechanical Systems, Journal of*, vol. 9, pp. 262-269, 2000.

[11] J. E. Mehner, L. D. Gabbay, and S. D. Senturia, "Computer-aided generation of nonlinear reduced-order dynamic macromodels. II. Stress-stiffened case," *Microelectromechanical Systems, Journal of*, vol. 9, pp. 270-278, 2000.

[12] M. I. Younis, E. M. Abdel-Rahman, and A. Nayfeh, "A reduced-order model for electrically actuated microbeam-based MEMS," *Microelectromechanical Systems, Journal of*, vol. 12, pp. 672-680, 2003.

[13] N. J. Falkiewicz and C. E. S. Cesnik, "Proper orthogonal decomposition for reduced-order thermal solution in hypersonic aerothermoelastic simulations," *AIAA Journal*, vol. 49, pp. 994-1009, 2011.

[14] R. Perez, X. Q. Wang, A. Matney, and M. P. Mignolet, "Reduced Order Model For the Geometric Nonlinear Response of Complex Structures," presented at the ASME 2012 International Design Engineering Technical Conferences IDETC/CIE, Chicago, Illinois, 2012.

[15] C.-C. Chu and M. H. Milman, "Eigenvalue error analysis of viscously damped structures using a Ritz reduction method," *AIAA Journal*, vol. 30, pp. 2935-2944, 1992/12/01 1992.

[16] M. H. Milman and C.-C. Chu, "Optimization methods for passive damper placement and tuning," *Journal of Guidance, Control, and Dynamics*, vol. 17, pp. 848-856, 1994/07/01 1994.

[17] D. T. Griffith and D. J. Segalman, "Finite Element Calculations Illustrating a Method of Model Reduction for the Dynamics of Structures with Localized Nonlinearities," Sandia National Laboratories SAND2006-5843, 2006.

[18] D. J. Segalman, M. R. Brake, L. A. Bergman, A. F. Vakakis, and K. Willner, "Epistemic and Aleatoric Uncertainty in Modeling," presented at the ASME 2013 International Design Engineering Technical Conferences IDETC, Portland, Oregon, 2013.

[19] G. Kerschen, M. Peeters, J. C. Golinval, and A. F. Vakakis, "Nonlinear normal modes. Part I. A useful framework for the structural dynamicist," *Mechanical Systems and Signal Processing*, vol. 23, pp. 170-94, 2009.

[20] A. F. Vakakis, "Non-linear normal modes (NNMs) and their applications in vibration theory: an overview," *Mechanical Systems and Signal Processing*, vol. 11, pp. 3-22, 1997.

[21] R. D. Cook, D. S. Malkus, M. E. Plesha, and R. J. Witt, *Concepts and Applications of Finite Element Analysis*, Fourth ed.: John Wiley and Sons, 2002.

[22] R. J. Kuether and M. S. Allen, "Computing Nonlinear Normal Modes using Numerical Continuation and Force Appropriation," presented at the ASME 2012 International Design Engineering Technical Conferences IDETC/CIE, Chicago, Illinois, 2012.

[23] M. Peeters, G. Kerschen, and J. C. Golinval, "Dynamic testing of nonlinear vibrating structures using nonlinear normal modes," *Journal of Sound and Vibration*, vol. 330, pp. 486-509, 2011.

[24] M. Peeters, G. Kerschen, and J. C. Golinval, "Modal testing of nonlinear vibrating structures based on nonlinear normal modes: Experimental demonstration," *Mechanical Systems and Signal Processing*, vol. 25, pp. 1227-1247, 2011.

[25] M. S. Allen and R. J. Kuether, "Substructuring with Nonlinear Subcomponents: A Nonlinear Normal Mode Perspective," presented at the 30th International Modal Analysis Conference (IMAC XXX), Jacksonville, Florida, 2012.
[26] R. J. Kuether and M. S. Allen, "Structural Modification of Nonlinear FEA Subcomponents Using Nonlinear Normal Modes," presented at the 31st International Modal Analysis Conference (IMAC XXXI), Garden Grove, California, 2013.
[27] R. J. Kuether and M. S. Allen, "Nonlinear Modal Substructuring of Systems with Geometric Nonlinearities," in *54th AIAA/ASME/ASCE/AHS/ASC Structures, Structural Dynamics, and Materials Conference*, Boston, Massachusetts, 2013.
[28] M. Peeters, R. Viguié, G. Sérandour, G. Kerschen, and J. C. Golinval, "Nonlinear normal modes, Part II: Toward a practical computation using numerical continuation techniques," *Mechanical Systems and Signal Processing*, vol. 23, pp. 195-216, 2009.
[29] H. A. Ardeh and M. S. Allen, "Investigating Cases of Jump Phenomena in a Nonlinear Oscillatory System," presented at the 31st International Modal Analysis Conference (IMAC XXXI), Garden Grove, California, 2013.
[30] M. A. Crisfield, *Nonlinear finite element analysis of solids and structures. Volume 2: Advanced Topics*, 1991.
[31] J. D. Schoneman, M. S. Allen, and R. J. Kuether, "Are Nonlinear Normal Modes Useful for Predicting Response to Random Inputs?," in *55th AIAA/ASME/ASCE/AHS/ASC Structures, Structural Dynamics, and Materials Conference*, National Harbor, Maryland, 2014.
[32] S. W. Shaw and C. Pierre, "Normal Modes for Non-Linear Vibratory Systems," *Journal of Sound and Vibration*, vol. 164, pp. 85-124, 1993.
[33] L. Renson and G. Kerschen, "Nonlinear Normal Modes of Nonconservative Systems," presented at the 31st International Modal Analysis Conference (IMAC XXXI), Garden Grove, California, 2013.
[34] D. J. Segalman, "A Four-Parameter Iwan Model for Lap-Type Joints," *Journal of Applied Mechanics*, vol. 72, pp. 752-760, September 2005.